Computation of the effective slip of rough hydrophobic surfaces via homogenization

Matthieu Bonnivard, Anne-Laure Dalibard, David Gérard-Varet

Computation of the effective slip of rough hydrophobic surfaces *via* homogenization

*Matthieu Bonnivard, †Anne-Laure Dalibard and ‡David Gérard-Varet

Abstract

We present a quantitative analysis of the effect of rough hydrophobic surfaces on viscous newtonian flows. We use a model introduced by Ybert and coauthors in [17], in which the rough surface is replaced by a flat plane with alternating small areas of slip and no-slip. We investigate the averaged slip generated at the boundary, depending on the ratio between these areas. This problem reduces to the homogenization of a non-local system, involving the Dirichlet to Neumann map of the Stokes operator, in a domain with small holes. Pondering on the works [2, 3], we compute accurate scaling laws of the averaged slip for various types of roughness (riblets, patches). Numerical computations complete and confirm the analysis.

1 Introduction

With the development of microfluidics, drag reduction for low Reynolds number flows, notably at solid walls, has become a stimulating issue. Therefore, the interaction between a fluid and a solid boundary has been investigated thoroughly, both at the experimental and theoretical levels. A special attention has been paid to the detection of slip, for various types of flows and solid walls. We refer to [13] for a review.

As a result of this activity, the idea that *rough boundaries could generate a substantial slip* has spread out. This idea has developped on the basis of both experimental and theoretical works, notably on *wall laws*. We remind that in the context of roughness effects, a wall law is an effective boundary condition imposed at a smoothened boundary, reflecting the overall impact of the real rough boundary. In particular, if one describes the rough boundary through an oscillation of small amplitude and wavelength ϵ, one can show rigorously that a no-slip condition at the rough boundary can be replaced by a wall law of Navier type, with slip length of order ϵ. We refer for instance to [1, 12, 5] for more precise statements.

However, these seemingly favorable results must be considered with care. For instance, at the experimental level, one must ensure that the slip is not measured too much away from the boundary. Also, as regards the theoretical works on wall laws, *the position of the artificial boundary at which the law is prescribed is crucial*. In particular, all forementioned works consider artifical boundaries that are at the top of the roughness. As a result, the flow

*Univ. Paris Diderot, Sorbonne Paris Cité, Laboratoire Jacques-Louis Lions, UMR 7598, UPMC, CNRS, F-75205 Paris, FRANCE.

†DMA/CNRS, Ecole Normale Supérieure, 45 rue d'Ulm, 75005 Paris, FRANCE, tel: +33 1 44 32 20 58, fax: +33 1 44 32 20 80.

‡IMJ and University Paris 7, 175 rue du Chevaleret, 75013 Paris.

rate in the smoothened domain does not equal the averaged flow rate in the rough domain, making comparisons inaccurate. This is the issue of the so-called apparent slip, noticed in []. In fact, in the case of rough wetting surfaces (endowed with a no-slip condition), one can even show the following: if one puts the artificial boundary in a way that the flow rates are the same, *then the flat boundary is optimal with respect to drag minimization.* We refer to [6] for detailed statements and proofs. Hence, the possibility of decreasing drag through roughness is not so clear, especially for rough wetting surfaces.

Still, in the recent years, promising results have been obtained concerning a class of rough hydrophobic surfaces, see for instance [16]. Indeed, by the combination of the chemical and geometrical properties of these surfaces, the hollows of the roughness get filled with gas. Hence, the viscous fluid above does not penetrate: it slips above the hollows, and only sticks at the bumps, reaching the so-called *Cassie or fakir state.*

The aim of this paper is to study the slip generated by such configurations, both in a rigorous and quantitative manner. We focus on a model proposed in article [17], in which the rough boundary is replaced by a flat plane, divided in small periodic cells (say of side $\epsilon \ll 1$). Each cell is divided in two zones:

- A no-slip zone, corresponding to a plane projection of the sticky part of the roughness (bumps).
- A slip-zone, corresponding to a plane projection of the slippery part.

Using homogenization techniques, we derive an effective boundary condition as ϵ goes to zero, depending on the size a^ϵ of the no-slip zones. We provide in this way scaling laws for the slip coefficients, for various configurations (patches, riblets). Such laws are in global agreement with the formal computations led in [17]. *One shows notably that the riblet configuration is less effective than patches one (see Remark 3).* All our theoretical results are grounded by numerical computations at the end of the paper.

2 Main results

Let us first present the model under study. We consider a three-dimensional Stokes flow between two infinite plates:

$$\begin{aligned} -\Delta u + \nabla p &= f \quad \text{in } \Omega, \\ \text{div } u &= 0 \quad \text{in } \Omega, \end{aligned} \tag{2.1}$$

where $\Omega = \mathbb{T}^2 \times (0,1)$ and $\mathbb{T}^2 = \mathbb{R}^2/\mathbb{Z}^2$. We denote by $x = (x_1, x_2, x_3) = (x_h, x_3)$ the space variable. The function $f \in L^2(\Omega)$ is a given source term. On the upper surface $x_3 = 1$, we enforce a "no-slip" boundary condition

$$u_{|x_3=1} = 0. \tag{2.2}$$

On the lower surface, we assume that u satisfies alternately "perfect slip" and "no slip" boundary conditions, corresponding respectively to the hollows and bumps of the rough hydrophobic surface. More precisely, let $\epsilon > 0$ and

$$S^\epsilon := [0,\epsilon)^2 \ \sim \ \left(\mathbb{R}/\left(\epsilon\mathbb{Z}\right)\right)^2,$$

the elementary square of side ϵ . For simplicity, we shall assume all along that ϵ^{-1} is an integer. Let T^ϵ be a Lipschitz subdomain of S^ϵ, modeling an elementary no-slip zone. Details about T^ϵ will be given right below. From this elementary no-slip zone, we define a global one inside $[0,1)^2 \sim \mathbb{T}^2$:

$$\mathcal{T}^\epsilon := \bigcup_{k\in[|0,\dots,\epsilon^{-1}|]^2} (\epsilon k + T^\epsilon)\,.$$

Finally, the boundary condition at $x_3 = 0$ is

$$u_{3|x_3=0} = 0, \quad \partial_3 u_{h|x_3=0} = 0 \text{ on } (\mathcal{T}^\epsilon)^c \times \{0\}, \quad u_{h|x_3=0} = 0 \text{ on } \mathcal{T}^\epsilon \times \{0\}. \tag{2.3}$$

It is easily proved that (2.1)-(2.2)-(2.3) has a unique solution $(u^\epsilon, p^\epsilon) \in H^1(\Omega) \times L^2(\Omega)/\mathbb{R}$.

This article is devoted to the asymptotic analysis of (u^ϵ, p^ϵ), as $\epsilon \to 0$. We will distinguish between two types of no-slip pattern T^ϵ:

- **Patches:** we assume that
$$T^\epsilon := (\frac{\epsilon}{2}, \frac{\epsilon}{2}) + a_\epsilon T, \tag{2.4}$$
where $(\frac{\epsilon}{2}, \frac{\epsilon}{2})$ is the center of the square S^ϵ, and where the domain T is relatively compact in $(-1/2, 1/2)^2$, and contains a disk of radius $\alpha > 0$, centered in the origin (see Figure 1). The parameter a_ϵ is a positive number such that $a_\epsilon < \epsilon$. In this case, the no-slip zone is a union of periodically distributed patches.

- **Riblets:** we assume that
$$T^\epsilon := (\epsilon\mathbb{T}) \times (\frac{\epsilon}{2} + a_\epsilon I). \tag{2.5}$$
where $I \subset (-\frac{1}{2}, \frac{1}{2})$ is an open interval (see Figure 2). In this case, the no-slip zone is a union of stripes, invariant in the x_1-direction. Of course, invariance in the x_2 direction could have been considered as well. Note that later on, addressing the case of riblets, we shall focus on two particular cases:
  - $f = e_1$: riblets parallel to the flow;
  - $f = e_2$: riblets perpendicular to the flow.

The issue is to derive a wall law for the system (2.1)-(2.2)-(2.3), that is, to replace the mixed boundary condition (2.3) at $x_3 = 0$ by a condition which does not depend on ϵ. We will show that u^ϵ behaves asymptotically like the solution $\bar{u}$ in H^1 of (2.1)-(2.2), endowed either with a Navier boundary condition

$$u_3 = 0 \text{ at } x_3 = 0, \quad \partial_3 u_h = M u_h \text{ at } x_3 = 0, \tag{2.6}$$

or with a Dirichlet boundary condition

$$u_{|x_3=0} = 0. \tag{2.7}$$

In (2.6), M is a 2×2 non-negative matrix, whose eigenvalues have the dimension of the inverse of a length. If $M = \lambda \mathrm{Id}$, the number λ^{-1} is called the "slip length". In the general case, the inverse of the eigenvalues provide the slip lengths in the directions of the eigenvectors. We shall denote $\bar{u}_M$ the solution of (2.1)-(2.2)-(2.6). We will write $\bar{u}_0$ in the special case $M = \left(\begin{smallmatrix} 0 & 0 \\ 0 & 0 \end{smallmatrix}\right)$. Eventually, we shall denote $\bar{u}_\infty$ the solution of (2.1)-(2.2)-(2.7).

With the previous notation, we can state our first result:

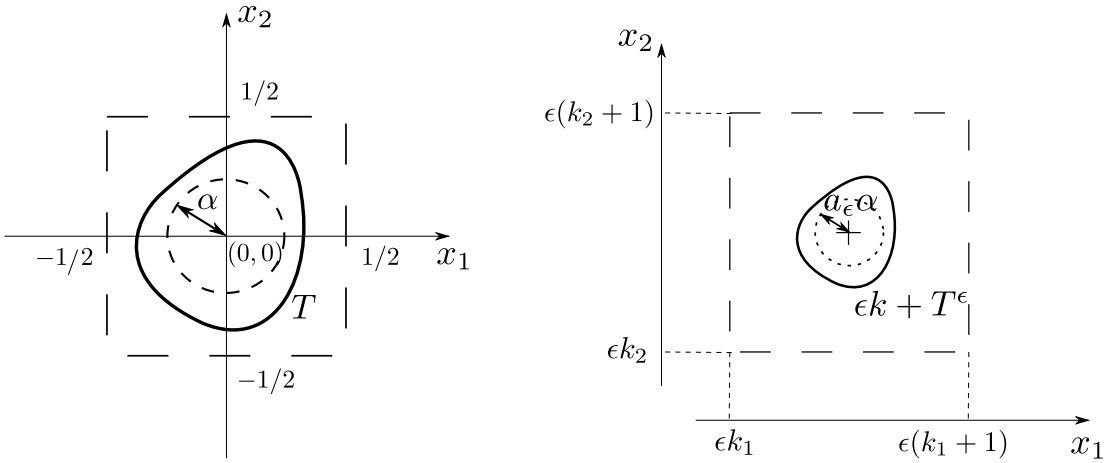

Figure 1: Patch configuration. For every $k = (k_1, k_2) \in [|0, \dots, \epsilon^{-1}|]^2$, the intersection of the no-slip zone $\mathcal{T}^\epsilon$ with the cell $[\epsilon k_1, \epsilon(k_1+1)) \times [\epsilon k_2, \epsilon(k_2+1))$ is defined by $\epsilon k + T^\epsilon = \epsilon k + a_\epsilon T$.

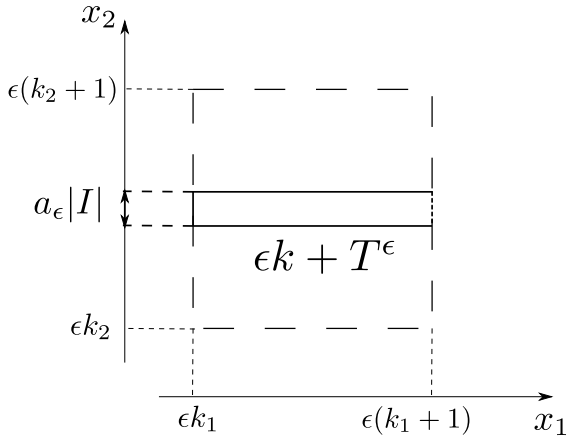

Figure 2: Riblet configuration. For $k = (k_1, k_2)$, the intersection of the no-slip zone $\mathcal{T}^\epsilon$ with the cell $[\epsilon k_1, \epsilon(k_1+1)) \times [\epsilon k_2, \epsilon(k_2+1))$ is defined by $\epsilon k + T^\epsilon = \epsilon k + (\epsilon\mathbb{T}) \times (\frac{\epsilon}{2} + a_\epsilon I)$.

Theorem 1. *(Asymptotic behavior for patches)*

Assume that $T^\epsilon := (\frac{\epsilon}{2}, \frac{\epsilon}{2}) + a_\epsilon T$. *Let* $u^\epsilon \in H^1(\mathbb{T}^2 \times (0,1))$ *be the solution of* (2.1), (2.2), (2.3). *One must distinguish between three cases:*

1. *Sub-critical case: if* $a_\epsilon \ll \epsilon^2$, *then* $u^\epsilon \rightharpoonup \bar{u}_0$ *in* $H^1(\mathbb{T}^2 \times (0,1))$;
2. *Super-critical case: if* $a_\epsilon \gg \epsilon^2$, *then* $u^\epsilon \rightharpoonup \bar{u}_\infty$ *in* $H^1(\mathbb{T}^2 \times (0,1))$;
3. *Critical case: there exists a symmetric, positive definite matrix* M_0 *such that if* $a_\epsilon/\epsilon^2 \to C_0 > 0$, *then* $u^\epsilon \rightharpoonup \bar{u}_{C_0 M_0}$ *in* $H^1(\mathbb{T}^2 \times (0,1))$.

A similar result holds for riblets. Let us merely state the theorem in the critical case:

Theorem 2. *(Asymptotic behaviour for riblets)*

Assume that $T^\epsilon := (\epsilon\mathbb{T}) \times (a_\epsilon I)$. *Suppose that* $\lim_{\epsilon\to 0} -\epsilon \ln(a_\epsilon) = C_0 > 0$, *and furthermore that* f *does not depend on* x_1.

Then, $u^\epsilon \rightharpoonup \bar{u}_{M_{rib}}$, *where*

$$M_{rib} = \begin{pmatrix} \frac{\pi}{C_0} & 0 \\ 0 & \frac{2\pi}{C_0} \end{pmatrix}. \tag{2.8}$$

Additionally, when $f = e_1$ *or* $f = e_2$, *the limit system can be simplified:*

- *if* $f = e_1$ *(riblets parallel to the main flow), then* $\bar{u}_{M_{rib},2} = \bar{u}_{M_{rib},3} = 0$ *and* $\bar{u}_{M_{rib},1}$ *satisfies*
$$\partial_3 \bar{u}_{M_{rib},1} = \frac{\pi}{C_0} \bar{u}_{M_{rib},1} \quad \text{at } x_3 = 0.$$
Hence, the slip length is C_0/π;
- *if* $f = e_2$ *(riblets perpendicular to the main flow), then* $\bar{u}_{M_{rib},1} = 0$ *and* $\bar{u}_{M_{rib},2}$ *satisfies*
$$\partial_3 \bar{u}_{M_{rib},2} = \frac{2\pi}{C_0} \bar{u}_{M_{rib},2} \quad \text{at } x_3 = 0.$$
Hence, the slip length is $C_0/(2\pi)$.

Remark 3. *Notice that theorems 1 and 2 indicate that for a given area of no-slip, riblets are less efficient than patches in terms of slip optimization. Indeed, consider riblets* T^ϵ *with area* ϵa_ϵ *corresponding to the critical case in Theorem 2* $\lim_{\epsilon\to 0} -\epsilon \ln(a_\epsilon) = C_0 > 0$. *Patches with the same area have a diameter of order* $\sqrt{\epsilon a_\epsilon}$: *they have a sub-critical behavior (with regards to Theorem 1) since* $\sqrt{\epsilon a_\epsilon} \ll \epsilon^2$. *So,* u^ϵ *converges towards* $\bar{u}_0$. *In other words, for the same area, patches achieve perfect slip on the lower surface, while riblets only have finite slip. In a similar fashion, it can be proved that riblets whose area* a_ϵ^2 *is critical for patches - i. e. such that* $a_\epsilon \sim \epsilon^2$, *see Theorem 1- have a super-critical behavior (with regards to Theorem 2) and converge towards* $\bar{u}_\infty$: *the solution satisfies a no-slip condition at the limit.*

Remark 4. *Our results are consistent with those of [17]: indeed, in the case of patches, it is shown heuristically there that the slip length is proportional to* ϵ^2/a_ϵ: *in other words, if* $a_\epsilon \ll \epsilon^2$, *perfect slip is achieved, if* $a_\epsilon \gg \epsilon^2$, *a no-slip condition is retrieved in the limit, and in the critical case, the slip length is positive and finite.*

Also, explicit calculations (see [14]) recalled in [17] show that the slip length for riblets is equal to $-\epsilon/\pi \ln(a_\epsilon/\epsilon)$ *for riblets parallel to the flow, and to* $-\epsilon/(2\pi)\ln(a_\epsilon/\epsilon)$ *for riblets perpendicular to the flow. Once again, this is consistent with Theorem 2.*

Remark 5. *Theorems 1 and 2 do not support the idea that rough hydrophobic surfaces can generate a substantial slip. Indeed, to obtain an effective slip law, the surface fraction of no-slip has to be very small. Back to wall roughness, this would correspond to narrow peaks separated by (comparatively) large hollows. It seems far from the roughness characteristics used experimentally to obtain a hydrophobic Cassie state.*

The proofs of theorems 1 and 2, that rely strongly on the papers [2, 3] by Allaire, are given in Section 3 and 4 respectively. We then present in Section 5 numerical simulations that confirm the asymptotic results, and clarify the influence of the shape of patches on the slip length, i.e. on the eigenvalues of the matrix M.

3 Asymptotic study of "patch" designs

This section is devoted to the proof of Theorem 1. Let $(u^\epsilon, p^\epsilon) \in H^1(\Omega) \times L^2(\Omega)/\mathbb{R}$ be the solution of (2.1), (2.2), (2.3). By classical arguments, the sequence (u^ϵ, p^ϵ) is uniformly bounded in $H^1(\Omega) \times L^2(\Omega)/\mathbb{R}$, and consequently, there exists a couple $(\overline{u}, \overline{p}) \in H^1(\Omega) \times L^2(\Omega)/\mathbb{R}$ such that

$$u^\epsilon \rightharpoonup \overline{u} \quad \text{weakly in } H^1(\Omega), \quad p^\epsilon \rightharpoonup \overline{p} \quad \text{weakly in } L^2(\Omega)/\mathbb{R}.$$

Using the weak formulation of Eqs. (2.1) and the continuity of the trace operator, one obtains easily that the weak-limit $(\overline{u}, \overline{p})$ satisfies Eqs. (2.1) and boundary condition (2.2) on $x_3 = 1$. On $x_3 = 0$, the boundary condition satisfied by the vertical component is preserved in the limit, and we obtain $\overline{u}_{3|x_3=0} = 0$. To describe the boundary condition satisfied by the horizontal components $(\overline{u}_1, \overline{u}_2)$ on $x_3 = 0$, we need to distinguish between the so-called super-critical, critical and sub-critical cases.

Notation. For every $k = (k_1, k_2) \in [|0, \epsilon^{-1}|]^2$, we denote the elementary squares, cubes and half-cubes as follows:

$$S_k^\epsilon := \epsilon k + S^\epsilon, \quad P_k^\epsilon := S_k^\epsilon \times (-\frac{\epsilon}{2}, \frac{\epsilon}{2}), \quad P_k^{\epsilon,+} := P_k^\epsilon \cap \mathbb{R}^3_+. \tag{3.1}$$

We shall use that notation throughout the paper.

Super-critical case: $a_\epsilon \gg \epsilon^2$. The proof in the super-critical case relies on a quantitative Poincaré inequality: we claim that there exist $\epsilon_0 > 0$ and a positive function $\eta(\epsilon)$ such that $\eta(\epsilon) \to 0$ as $\epsilon \to 0$, and such that

$$\int_{\mathbb{T}^2 \times \{0\}} |u^\epsilon|^2 \leq \eta(\epsilon) \int_\Omega |\nabla u^\epsilon|^2 \qquad \forall 0 < \epsilon < \epsilon_0. \tag{3.2}$$

We provide a proof of this inequality in the Appendix.

Since u^ϵ is bounded in $H^1(\Omega)$, we immediately infer that $\bar{u}_{|x_3=0}$ vanishes in $L^2(\mathbb{T}^2)$. Thus $(\bar{u}, \bar{p})$ is a solution of the Stokes system with homogeneous Dirichlet boundary conditions at $x_3 = 0$ and $x_3 = 1$, i.e. $\bar{u} = \bar{u}_\infty$.

Critical and sub-critical cases: $a_\epsilon \lesssim \epsilon^2$. We follow here the strategy of articles [2, 3] by Allaire. These articles deal with the homogenization of the Stokes equations across a network of balls, with a Dirichlet condition at the surface of the balls. Notably, in section

4 of [2], the balls are assumed to be distributed along a hypersurface (for instance, 3d balls with centers periodically located on a plane). In the setting considered here, the rough idea is to extend the Stokes solution to the lower half-space by appropriate symmetry: our problem is then reduced to the homogenization of the Stokes equations across a planar network of patches. Hence, the ideas of [2], devoted to a planar network of balls, essentially apply. They are based on the construction of correctors and the method of oscillating test functions. We start with

Lemma 6 (Existence of correctors)**.** *Assume that $a_\epsilon \lesssim \epsilon^2$. For every $\epsilon > 0$, there exist $W^\epsilon = (W^\epsilon_{i,j})_{1\le i,j\le 3} \in H^1(\Omega)^9$, $q^\epsilon = (q^\epsilon_j)_{1\le j\le 3} \in L^2(\Omega)^3$, supported in $\mathbb{T}^2 \times [-\epsilon/2, \epsilon/2]$, which satisfy the following properties:*

(i) $W^\epsilon \rightharpoonup 0$ weakly in $H^1(\Omega)$, $q^\epsilon \rightharpoonup 0$ weakly in $L^2(\Omega)$;

(ii) for every $j = 1 \dots 3$, $\sum_i \partial_i W^\epsilon_{ij} = 0$ in Ω;

(iii) for $1 \le i, j \le 3$, $W^\epsilon_{3j} = W^\epsilon_{i3} = 0$ on $\mathbb{T}^2 \times \{0\}$, and for $1 \le i, j \le 2$, $W^\epsilon_{ij} = \delta_{ij}$ on $\mathcal{T}^\epsilon \times \{0\}$;

(iv) For every $\phi \in C^\infty(\overline{\Omega})^3$, every $\psi \in H^1(\Omega)^3$ and every sequence $\psi^\epsilon \in H^1(\Omega)^3$ satisfying the boundary conditions

$$\psi^\epsilon = 0 \text{ on } (\mathcal{T}^\epsilon \times \{0\}) \cup (\mathbb{T}^2 \times \{1\}), \quad \psi^\epsilon_3 = 0 \text{ on } \mathbb{T}^2 \times \{0, 1\}, \tag{3.3}$$

and converging weakly to ψ in $H^1(\Omega)^3$, the following relation holds: if $\lim_{\epsilon\to 0} a_\epsilon/\epsilon^2 = C_0 \ge 0$, then

$$\lim_{\epsilon\to 0} \sum_{1\le i,j\le 3} \left(\int_\Omega \nabla W^\epsilon_{ij} \cdot \nabla \psi^\epsilon_i \phi_j - \int_\Omega \partial_i \psi^\epsilon_i q^\epsilon_j \phi_j \right) = -C_0 \int_{\mathbb{T}^2\times\{0\}} M_0 \psi_h \cdot \phi_h. \tag{3.4}$$

where $M_0 \in \mathcal{M}_2(\mathbb{R})$ is the symmetric definite positive matrix given by formula (3.19)*.*

Proof of Lemma 6. This lemma is the analogue of Proposition 4.1.6 in [3] (see also section 2.3 in [2]). As mentioned before, we do not claim any major novelty in the proof. Nevertheless, with regards to quantitative aspects, notably the exact expression of the slip matrix $C_0\, M_0$, we feel necessary to reproduce its main steps.

The starting idea is to consider a base flow (W, q) in the vicinity of T, which, after proper rescaling, will describe accurately the corrector behavior near a single patch. We shall then truncate it and periodize so as to obtain an appropriate global corrector. Namely, we introduce the solution (W, q), with $W = (W_{ij})_{1\le i,j\le 3}$, $q = (q_i)_{1\le i\le 3}$, of the following problem:

$$-\Delta W_{ij} + \partial_i q_j = 0 \quad \text{in } \mathbb{R}^3_+,\ 1 \le i, j \le 3, \tag{3.5}$$

$$\sum_{i=1}^3 \partial_i W_{ij} = 0 \quad \text{in } \mathbb{R}^3_+,\ 1 \le j \le 3, \tag{3.6}$$

completed with the boundary conditions

$$W_{ij} = \delta_{ij} \quad \text{on } T \times \{0\},\ 1 \le i, j \le 2, \tag{3.7}$$

$$W_{i3} = W_{3j} = 0 \quad \text{on } \mathbb{R}^2 \times \{0\},\ 1 \le i, j \le 3, \tag{3.8}$$

$$\partial_3 W_{ij} = 0 \quad \text{on } (\mathbb{R}^2 \setminus T) \times \{0\},\ 1 \le i, j \le 2. \tag{3.9}$$

as well as $\lim_{|x|\to\infty} W = 0$. Of course, for $j = 3$, we have $W_{i3} \equiv 0$ and $q_3 \equiv 0$. For $j = 1, 2$, the existence of a unique weak solution

$$(W_{\cdot j}, q_j) \in \left(D^{1,2}(\mathbb{R}^3_+)\right)^3 \times L^2_{loc}(\mathbb{R}^3_+)/\mathbb{R}$$

follows from Lax-Milgram theorem. Following [9], we remind that $D^{1,2}(\mathbb{R}^3_+)$ is the closure of $\mathcal{D}(\overline{\mathbb{R}^3_+})$ in $\dot{H}^1(\mathbb{R}^3_+)$.

Asymptotic behaviour of W_{ij}, q_j. For $j = 1 \dots 3$, we extend q_j, W_{1j} and W_{2j} into even functions of x_3, and W_{3j} into an odd function of x_3. We obtain in this way solutions of the Stokes equations on $\mathbb{R}^3 \setminus T$. Proceeding exactly as in [2, p. 255], we obtain the following asymptotic expansions

$$W_{\cdot j}(x) = \frac{1}{8\pi}\left(\frac{F_j}{|x|} + \frac{(x \cdot F_j)x}{|x|^3}\right) + O(\frac{1}{|x|^2}) \quad \text{as } |x| \to \infty. \tag{3.10}$$

$$q_j(x) = \frac{1}{4\pi}\frac{x \cdot F_j}{|x|^3} + O(\frac{1}{|x|^3}) \quad \text{as } |x| \to \infty, \tag{3.11}$$

In formulas (3.10)-(3.11), the notation F_j corresponds to the drag force, which is defined by (here, $n_+ := e_3$, $n_- := -e_3$):

$$\begin{aligned} F_j &= -\int_{T\times\{0^+\}} \frac{\partial W_{\cdot j}}{\partial n_+} - \int_{T\times\{0^-\}} \frac{\partial W_{\cdot j}}{\partial n_-} + \int_{T\times\{0^+\}} q_j n_+ + \int_{T\times\{0^-\}} q_j n_- \\ &= -2\int_{T\times\{0^+\}} \partial_3 W_{\cdot j}. \end{aligned} \tag{3.12}$$

Construction of W^ϵ and q^ϵ. Using the extended W and q, defined in the whole of $\mathbb{R}^3$, we can then proceed exactly as in [2, 3] to construct the correctors W^ϵ and q^ϵ. Therefore, we consider the following decomposition of P^ϵ_k (see definition (3.1)):

$$\overline{P^\epsilon_k} = C^\epsilon_k \cup \overline{D^\epsilon_k} \cup \overline{K^\epsilon_k},$$

where C^ϵ_k is the ball of radius $\epsilon/4$ centered in the cube, D^ϵ_k is the ball of radius $\epsilon/2$, with same center, perforated by C^ϵ_k, and K^ϵ_k is the remaining part of the cube, that is $K^\epsilon_k = P^\epsilon_k \setminus \overline{D^\epsilon_k}$ (see Figure 3). We denote by c^ϵ_k the center of cube P^ϵ_k. In each part of the cube, we define $W^\epsilon_{\cdot j}$ and q^ϵ_j as follows:

$$\begin{cases} W^\epsilon_{\cdot j}(x) = W_{\cdot j}(\frac{x-c^\epsilon_k}{a_\epsilon}) \\ q^\epsilon_j(x) = \frac{1}{a_\epsilon} q_j(\frac{x-c^\epsilon_k}{a_\epsilon}) \end{cases} \forall x \in C^\epsilon_k, \ , \begin{cases} \nabla q^\epsilon_j - \Delta W^\epsilon_{\cdot j} = 0 \\ \text{div } W^\epsilon_{\cdot j} = 0 \end{cases} \text{in } D^\epsilon_k, \qquad \begin{cases} W^\epsilon_{\cdot j} = 0 \\ q^\epsilon_j = 0 \end{cases} \text{in } K^\epsilon_k.$$

Moreover, we impose $\int_{D^\epsilon_k} q^\epsilon_j = 0$ and $W^\epsilon_{\cdot j} \in H^1(P^\epsilon_k)^3$ (so that there is no jump of W^ϵ across ∂D^ϵ_k, ∂C^ϵ_k).

Estimates on W^ϵ and q^ϵ. We use again the decomposition $P^\epsilon_k = C^\epsilon_k \cup (P^\epsilon_k \setminus \overline{C^\epsilon_k})$. The estimates in C^ϵ_k follow from the asymptotic expansions (3.10)-(3.11) and a scaling argument: for every $\epsilon > 0$,

$$\|\nabla W^\epsilon_{\cdot j}\|^2_{L^2(C^\epsilon_k)} \le C a_\epsilon, \ \|q^\epsilon_j\|_{L^2(C^\epsilon_k)} \le C a_\epsilon, \ \|W^\epsilon_{\cdot j}\|^2_{L^2(C^\epsilon_k)} \le C a^2_\epsilon \epsilon,$$

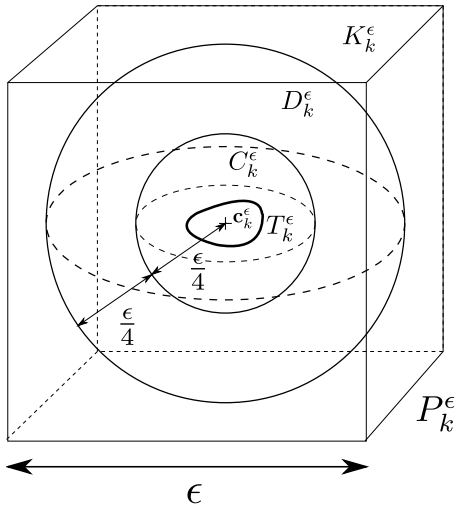

Figure 3: Each cube P_k^ϵ is decomposed into a union of subdomains C_k^ϵ, D_k^ϵ and K_k^ϵ, which separated by spheres of radius $\epsilon/4$ and $\epsilon/2$ centered in the cube.

where $C > 0$ is a constant. To treat the remaining part $P_k^\epsilon \setminus \overline{C_k^\epsilon}$, we use a properly rescaled version of standard estimates for the homogeneous Stokes equations: basically, the L^2 norm, resp. H^1 norm of the solution is controlled by the L^2 norm, resp. $H^{1/2}$ norm of the boundary data (see for instance [15]). Since the velocity fields $W_{\cdot j}^\epsilon$ satisfy the following pointwise asymptotics as ϵ vanishes

$$W_{\cdot j}^\epsilon = O\left(\frac{a_\epsilon}{\epsilon}\right) \quad \text{on } \partial C_k^\epsilon \cap \partial D_k^\epsilon, \qquad \nabla W_{\cdot j}^\epsilon = O\left(\frac{a_\epsilon}{\epsilon^2}\right) \quad \text{on } \partial C_k^\epsilon \cap \partial D_k^\epsilon,$$

using a scaling argument, we obtain the following estimates

$$\|\nabla W_{\cdot j}^\epsilon\|^2_{L^2(P_k^\epsilon \setminus \overline{C_k^\epsilon})} \leq C\frac{a_\epsilon^2}{\epsilon}, \ \|q_j^\epsilon\|_{L^2(P_k^\epsilon \setminus \overline{C_k^\epsilon})} \leq C\frac{a_\epsilon^2}{\epsilon}, \ \|W_{\cdot j}^\epsilon\|^2_{L^2(P_k^\epsilon \setminus \overline{C_k^\epsilon})} \leq C a_\epsilon^2 \epsilon, \tag{3.13}$$

for a given constant $C > 0$. Since $0 < a_\epsilon < \epsilon$, we deduce

$$\|\nabla W_{\cdot j}^\epsilon\|^2_{L^2(P_k^\epsilon)} \leq C a_\epsilon, \ \|q_j^\epsilon\|_{L^2(P_k^\epsilon)} \leq C a_\epsilon, \ \|W_{\cdot j}^\epsilon\|^2_{L^2(P_k^\epsilon)} \leq C a_\epsilon^2 \epsilon.$$

As a result, summing over $k \in [|0, \epsilon^{-1}|]^2$, we obtain the following asymptotics as ϵ vanishes

$$\|\nabla W^\epsilon\|^2_{L^2(\Omega)} = O\left(\frac{a_\epsilon}{\epsilon^2}\right), \quad \|q^\epsilon\|_{L^2(\Omega)} = O\left(\frac{a_\epsilon}{\epsilon^2}\right), \quad \|W^\epsilon\|^2_{L^2(\Omega)} = O\left(\frac{a_\epsilon^2}{\epsilon}\right). \tag{3.14}$$

Conclusion of the proof. Let $\phi \in C^\infty(\overline{\Omega})^3$, $\psi \in H^1(\Omega)^3$ and let $\psi^\epsilon \in H^1(\Omega)^3$ be a sequence of vector fields satisfying the boundary conditions (3.3), and converging weakly to ψ in $H^1(\Omega)^3$. In the sub-critical case $a_\epsilon \ll \epsilon^2$, the asymptotics (3.14) imply that

$$W^\epsilon \to 0 \quad \text{strongly in } H^1(\Omega)^9, \quad q^\epsilon \to 0 \quad \text{strongly in } L^2(\Omega).$$

Consequently, the following relation holds:

$$\lim_{\epsilon \to 0} \sum_{1 \leq i,j \leq 3} \left(\int_\Omega \nabla W_{ij}^\epsilon \cdot \nabla \psi_i^\epsilon \phi_j - \int_\Omega \partial_i \psi_i^\epsilon q_j^\epsilon \phi_j \right) = 0.$$

Thus, relation (3.4) holds with $\overline{M} = 0$.

In the critical case $\lim_{\epsilon\to 0} \frac{a_\epsilon}{\epsilon^2} = C_0 > 0$, we define $\tilde{\Omega} = \mathbb{T}^2 \times (-1, 1)$, and we extend ϕ_j and ψ_j^ϵ into even functions of x_3 on $\tilde{\Omega}$ for $j = 1, 2$, and ϕ_3 and ψ_3 into odd functions of x_3. First, asymptotics (3.14) imply that W^ϵ is bounded in H^1, and therefore converges weakly in H^1, up to a subsequence. Since W^ϵ vanishes in $L^2(\Omega)$, we obtain $\nabla W^\epsilon \rightharpoonup 0$ weakly in $L^2(\Omega)^9$. From (3.14), we also infer $q_j^\epsilon \rightharpoonup 0$ weakly in $L^2(\Omega)$, and thus the following identity holds for every $1 \leq i \leq 3$, $1 \leq j \leq 2$

$$\begin{aligned}\int_\Omega \nabla W_{ij}^\epsilon \cdot \nabla \psi_i^\epsilon \phi_j - q_j^\epsilon (\partial_i \psi_i^\epsilon)\phi_j &= \frac{1}{2}\int_{\tilde{\Omega}} \nabla W_{ij}^\epsilon \cdot \nabla \psi_i^\epsilon \phi_j - q_j^\epsilon (\partial_i \psi_i^\epsilon)\phi_j \\ &= \frac{1}{2}\int_{\tilde{\Omega}} \nabla W_{ij}^\epsilon \cdot \nabla (\psi_i^\epsilon \phi_j) - q_j^\epsilon \partial_i(\psi_i^\epsilon \phi_j) + o(1), \quad \text{as } \epsilon \to 0.\end{aligned}$$

Moreover,

$$\begin{aligned}&\int_{\tilde{\Omega}} \nabla W_{ij}^\epsilon \cdot \nabla(\phi_j \psi_i^\epsilon) - q_j^\epsilon \partial_i(\phi_j \psi_i^\epsilon) = \sum_k \int_{P_k^\epsilon} \nabla W_{ij}^\epsilon \cdot \nabla(\phi_j \psi_i^\epsilon) - q_j^\epsilon \partial_i(\phi_j \psi_i^\epsilon) \\ =&\sum_k \int_{C_k^{\epsilon,+}} \nabla W_{ij}^\epsilon \cdot \nabla(\phi_j \psi_i^\epsilon) - q_j^\epsilon \partial_i(\phi_j \psi_i^\epsilon) \\ +&\sum_k \int_{C_k^{\epsilon,-}} \nabla W_{ij}^\epsilon \cdot \nabla(\phi_j \psi_i^\epsilon) - q_j^\epsilon \partial_i(\phi_j \psi_i^\epsilon) + \sum_k \int_{P_k^\epsilon \setminus C_k^\epsilon} \nabla W_{ij}^\epsilon \cdot \nabla(\phi_j \psi_i^\epsilon) - q_j^\epsilon \partial_i(\phi_j \psi_i^\epsilon),\end{aligned}$$

where $C_k^{\epsilon,\pm} = C_k^\epsilon \cap \mathbb{R}^3_\pm$. In all sums, k ranges over $[|0, \epsilon^{-1}|]^2$. Using the estimates (3.13), we infer that

$$\begin{aligned}\sum_k \int_{P_k^\epsilon \setminus C_k^\epsilon} \nabla W_{ij}^\epsilon \cdot \nabla(\phi_j \psi_i^\epsilon) - q_j^\epsilon \partial_i(\phi_j \psi_i^\epsilon) &\leq C\left(\|\nabla W^\epsilon\|_{L^2(\cup_k P_k^\epsilon \setminus C_k^\epsilon)} + \|q^\epsilon\|_{L^2(\cup_k P_k^\epsilon \setminus C_k^\epsilon)}\right) \\ &\leq C\left(\frac{a_\epsilon^2}{\epsilon}\frac{1}{\epsilon^2}\right)^{1/2} \ll 1.\end{aligned}$$

At this stage the proof differs slightly from the one of [3], because of the mixed boundary conditions at $x_3 = 0$. Indeed, since (W^ϵ, q^ϵ) satisfies the Stokes system in $C_k^{\epsilon,\pm}$, we have

$$\int_{C_k^{\epsilon,\pm}} \nabla W_{ij}^\epsilon \cdot \nabla(\phi_j \psi_i^\epsilon) - \int_{C_k^{\epsilon,\pm}} q_j^\epsilon \partial_i(\phi_j \psi_i^\epsilon) = \int_{\partial C_k^{\epsilon,\pm}} \left(\frac{\partial W_{ij}^\epsilon}{\partial n} - q_j^\epsilon n \cdot e_i\right)\phi_j \psi_i^\epsilon,$$

where n denotes the outer normal to the set $C_k^{\epsilon,\pm}$. In particular, due to the symmetry properties of $W^\epsilon, q^\epsilon, \phi, \psi^\epsilon$, there holds

$$\begin{aligned}&\int_{C_k^{\epsilon,+}} \nabla W_{ij}^\epsilon \cdot \nabla(\phi_j \psi_i^\epsilon) - \int_{C_k^{\epsilon,+}} q_j^\epsilon \partial_i(\phi_j \psi_i^\epsilon) + \int_{C_k^{\epsilon,-}} \nabla W_{ij}^\epsilon \cdot \nabla(\phi_j \psi_i^\epsilon) - \int_{C_k^{\epsilon,-}} q_j^\epsilon \partial_i(\phi_j \psi_i^\epsilon) \\ =&\int_{\partial C_k^\epsilon} \left(\frac{\partial W_{ij}^\epsilon}{\partial n} - q_j^\epsilon n \cdot e_i\right)\phi_j \psi_i^\epsilon - 2\int_{C_k^\epsilon \cap \{z=0\}} \partial_3 W_{ij}^\epsilon \phi_j \psi_i^\epsilon.\end{aligned}$$

By definition of W, $\partial_3 W_{ij}^\epsilon = 0$ on $(C_k^\epsilon \cap \{x_3 = 0\}) \setminus (\mathcal{T}^\epsilon \times \{0\})$. On the other hand, since ψ^ϵ satisfies (3.3), $\psi_i^\epsilon = 0$ on $\mathcal{T}^\epsilon \times \{0\}$. Therefore, the r.h.s. reduces to the integral on ∂C_k^ϵ.

Using the asymptotic expansions (3.10)-(3.11) and the expression of $W^\epsilon_{ij}, q^\epsilon_j$ in C^ϵ_k, we obtain, on ∂C^ϵ_k,

$$\frac{\partial W^\epsilon_{ij}}{\partial n} - q^\epsilon_j n \cdot e_i \;=\; -\frac{a_\epsilon}{\epsilon^2}\left[\frac{2}{\pi}F_{ij} + \frac{6}{\pi}F_j \cdot n_k n_k \cdot e_i\right] \;+\; \left(\frac{a_\epsilon}{\epsilon^2}\right)^2 \epsilon R^\epsilon_{ij},$$

where n_k is the unitary normal vector to the ball C^ϵ_k and R^ϵ_{ij} is a function of x, satisfying $R^\epsilon_{ij}(x) = O(1)$ as $\epsilon \to 0$, uniformly in x and k. This leads to the following decomposition

$$\begin{aligned}\int_{\tilde\Omega} \nabla W^\epsilon_{ij} \cdot \nabla(\phi_j \psi^\epsilon_i) - \int_{\tilde\Omega} q^\epsilon_j \partial_i(\phi_j \psi^\epsilon_i) = -\frac{a_\epsilon}{\epsilon^2}\sum_k \int_{\partial C^\epsilon_k}\left[\frac{2}{\pi}F_{ij} + \frac{6}{\pi}F_j \cdot n_k n_k \cdot e_i\right]\phi_j\psi^\epsilon_i \\ + \left(\frac{a_\epsilon}{\epsilon^2}\right)^2 \sum_k \int_{\partial C^\epsilon_k} \epsilon R^\epsilon_{ij}\phi_j\psi^\epsilon_i + o(1).\end{aligned}$$

Let $\delta_{\partial C^\epsilon_k}$ be the unit mass concentrated on ∂C^ϵ_k. Let us recall the following results, which are proved in [3] (see Lemma 4.2.1): the radius of the ball C^ϵ_k being equal to $\epsilon/4$, the following convergence holds[1]

$$\begin{aligned}\sum_k \delta_{\partial C^\epsilon_k} &\to \frac{\pi}{16}\delta_{\mathbb{T}^2\times\{0\}} \quad \text{strongly in } H^{-1}(\tilde\Omega), \\ \sum_k n_k n_k \cdot e_i \delta_{\partial C^\epsilon_k} &\to \frac{\pi}{48} e_i \delta_{\mathbb{T}^2\times\{0\}} \quad \text{strongly in } H^{-1}(\tilde\Omega).\end{aligned} \tag{3.15}$$

Let us write

$$\begin{aligned}\sum_k \int_{\partial C^\epsilon_k} \phi_j\psi^\epsilon_i &= \left\langle \sum_{k\in\mathcal{K}^\epsilon} \delta_{\partial C^\epsilon_k}, \phi_j\psi^\epsilon_i \right\rangle_{H^{-1}(\tilde\Omega)\times H^1_0(\tilde\Omega)}, \\ \sum_k \int_{\partial C^\epsilon_k} n_k n_k \cdot e_i \phi_j\psi^\epsilon_i &= \left\langle \sum_k n_k n_k \cdot e_i \delta_{\partial C^\epsilon_k}, \phi_j\psi^\epsilon_i \right\rangle_{H^{-1}(\tilde\Omega)\times H^1_0(\tilde\Omega)};\end{aligned} \tag{3.16}$$

consequently, since $\phi_j\psi^\epsilon_i \to \phi_j\psi_i$ weakly in $H^1(\tilde\Omega)$ and $\frac{a_\epsilon}{\epsilon^2} \to C_0$, we obtain

$$\lim_{\epsilon\to 0}\frac{a_\epsilon}{\epsilon^2}\sum_k \int_{\partial C^\epsilon_k}\left[\frac{2}{\pi}F_{ij} + \frac{6}{\pi}F_j \cdot n_k n_k \cdot e_i\right]\phi_j\psi^\epsilon_i = \frac{1}{4}C_0 \int_{\mathbb{T}^2\times\{0\}} F_{ij}\phi_j\psi_i. \tag{3.17}$$

Moreover, since R^ϵ_{ij} is uniformly bounded in $L^\infty(\tilde\Omega)$, pondering on the comparison principle of [2, Lemma 2.3.8] we deduce from (3.15) that

$$\epsilon\sum_k R^\epsilon_{ij}\delta_{\partial C^\epsilon_k} \to 0 \quad \text{strongly in } H^{-1}(\tilde\Omega).$$

Using (3.16), we obtain the following convergence:

$$\left(\frac{a_\epsilon}{\epsilon^2}\right)\sum_k \int_{\partial C^\epsilon_k} \epsilon R^\epsilon_{ij}\phi_j\psi^\epsilon_i \to 0 \quad \text{as } \epsilon \to 0. \tag{3.18}$$

[1]Notice that in the paper of Allaire, the periodicity of the pattern is 2ϵ, rather than ϵ as in the present paper. Hence the constant in front of the Dirac mass in the right-hand side is $\pi/16$, rather than $\pi/64$ for the first line, and $\pi/48$ rather than $\pi/192$ in the second line.

Gathering the convergence results (3.17)-(3.18), we obtain relation (3.4), where the matrix M_0 is defined by

$$M_{0,ij} \;=\; \frac{1}{8}F_{ij}, \quad F_{\cdot j} \;\; \text{given by (3.12)} \tag{3.19}$$

There only remains to prove that the matrix $(F_{ij})_{1\leq i,j\leq 2}$ is positive definite. To that end, we go back to system (3.5)-(3.9). We multiply by $W_{\cdot i}$ the system satisfied by $W_{\cdot j}$, and we obtain

$$F_{ij} = -2\int_{T\times\{0\}} \partial_3 W_{ij} = -2\int_{\mathbb{R}^3_+} \nabla W_{\cdot i} : \nabla W_{\cdot j}.$$

In particular, for all $\eta \in \mathbb{R}^2$,

$$\sum_{1\leq i,j\leq 2} \eta_i\eta_j F_{ij} = 2\int_{\mathbb{R}^3_+} |\nabla(\eta_1 W_{\cdot 1} + \eta_2 W_{\cdot 2})|^2 \geq 0,$$

and the right-hand side above vanishes if and only if $\eta_1 W_{\cdot 1} + \eta_2 W_{\cdot 2} = 0$ a.e. in $\mathbb{R}^3_+$. In view of the boundary conditions (3.7), this implies $\eta_1 = \eta_2 = 0$. This concludes the proof of Lemma 6.

□

To complete the proof of Theorem 1, we rely on Lemma 6, as follows. Let $\phi \in C^\infty(\overline{\Omega}^3)$ satisfying the no-slip condition $\phi = 0$ on the upper boundary $\mathbb{T}^2\times\{1\}$, and the non-penetration condition $\phi_3 = 0$ on the lower boundary $\mathbb{T}^2 \times \{0\}$. Let $W^\epsilon \in H^1(\Omega)^9$, $q^\epsilon \in L^2(\Omega)^3$ be the sequences introduced in Lemma 6. We define the following test functions for the weak formulation associated to system (2.1)-(2.3):

$$\phi^\epsilon = (\mathrm{I}_3 - W^\epsilon)\phi, \quad r^\epsilon = q^\epsilon\phi,$$

where I_3 is the identity matrix in $\mathcal{M}_3(\mathbb{R})$. We deduce the following relation:

$$\int_\Omega \nabla u^\epsilon : \nabla\phi^\epsilon - \int_\Omega p^\epsilon \mathrm{div}\ \phi^\epsilon = \int_\Omega f\phi^\epsilon \tag{3.20}$$

$$\int_\Omega r^\epsilon \mathrm{div}\ u^\epsilon = 0. \tag{3.21}$$

Since W^ϵ converges weakly to 0 in $H^1(\Omega)^9$, and strongly to 0 in $L^2(\Omega)^9$, we readily obtain

$$\begin{aligned}
\int_\Omega \nabla u^\epsilon : \nabla\phi^\epsilon &= \int_\Omega \nabla u^\epsilon : \nabla\phi - \int_\Omega \nabla u_i^\epsilon \nabla W_{ij}^\epsilon \phi_j - \int_\Omega \nabla u_i^\epsilon \nabla\phi_j W_{ij}^\epsilon \\
&= \int_\Omega \nabla\overline{u} : \nabla\phi - \int_\Omega \nabla u_i^\epsilon \nabla W_{ij}^\epsilon \phi_j + o(1), \quad \text{as } \epsilon\to 0, \\
-\int_\Omega p^\epsilon \mathrm{div}\ \phi^\epsilon &= -\int_\Omega p^\epsilon(\mathrm{I}_3 - W^\epsilon) : \nabla\phi \;=\; -\int_\Omega \overline{p}\ \mathrm{div}\ \phi + o(1), \quad \text{as } \epsilon\to 0.
\end{aligned}$$

Consequently, summing relations (3.20) and (3.21), we deduce the asymptotic relation

$$\int_\Omega \nabla\overline{u} : \nabla\phi - \int_\Omega \overline{p}\ \mathrm{div}\ \phi - \int_\Omega \nabla u_i^\epsilon \nabla W_{ij}^\epsilon \phi_j + \int_\Omega q^\epsilon\phi\ \mathrm{div}\ u^\epsilon = o(1), \quad \text{as } \epsilon\to 0.$$

Applying Lemma 6 with $\psi = \overline{u}$ and $\psi^\epsilon = u^\epsilon$, we obtain the following relation:

$$\int_\Omega \nabla \overline{u} : \nabla \phi - \int_\Omega \overline{p} \ \mathrm{div}\ \phi + C_0 \int_{\mathbb{T}^2 \times \{0\}} M_0 u \cdot \phi = 0, \tag{3.22}$$

where the matrix $M_0 \in \mathcal{M}_2(\mathbb{R})$ is defined by (3.19). Since relation (3.22) holds for every test function ϕ, this proves that $\overline{u} = \overline{u}_{C_0 M_0}$.

4 Asymptotic study of "riblet" designs

This section is devoted to the proof of Theorem 2. In the case of riblets, we recall that $\mathcal{T}^\epsilon$ is invariant by translation in x_1. Since $f = (f_1, f_2, f_3)$ is also independent on the x_1 variable, the solution (u^ϵ, p^ϵ) of system (2.1)-(2.2)-(2.3) depends only on (x_2, x_3). As a result, the first component of u^ϵ satisfies:

$$\begin{aligned} -\Delta_{2,3} u_1^\epsilon &= f_1 \quad \text{in } \mathbb{T} \times (0,1), \\ u_1^\epsilon &= 0 \quad \text{on } \mathbb{T} \times \{1\}, \\ \partial_3 u_1^\epsilon = 0 \text{ on } (\mathbb{T} \times \{0\}) \setminus (\Pi \mathcal{T}^\epsilon), &\quad u_1^\epsilon = 0 \text{ on } \Pi \mathcal{T}^\epsilon, \end{aligned} \tag{4.1}$$

where $\nabla_{2,3}$ and $\Delta_{2,3}$ stand for the gradient (resp. the Laplacian) with respect to the (x_2, x_3) variables, $\mathbb{T}^1 = \mathbb{R}/\mathbb{Z}$ and where we have denoted Π the projection operator defined by $\Pi(x_1, x_2, 0) = (x_2, 0)$. In the same fashion, $(u_2^\epsilon, u_3^\epsilon), p^\epsilon$ satisfy the following Stokes problem:

$$\begin{aligned} -\Delta_{2,3} \begin{pmatrix} u_2^\epsilon \\ u_3^\epsilon \end{pmatrix} + \nabla_{2,3} p^\epsilon &= \begin{pmatrix} f_2 \\ f_3 \end{pmatrix} \quad \text{in } \mathbb{T} \times (0,1), \\ \nabla_{2,3} \cdot \begin{pmatrix} u_2^\epsilon \\ u_3^\epsilon \end{pmatrix} &= 0 \quad \text{in } \mathbb{T} \times (0,1), \\ u_{2,3}^\epsilon &= 0 \quad \text{on } \mathbb{T} \times \{1\}, \\ u_3^\epsilon &= 0 \quad \text{on } \mathbb{T} \times \{0\}, \\ \partial_3 u_2^\epsilon = 0 \text{ on } (\mathbb{T} \times \{0\}) \setminus (\Pi T^\epsilon), &\quad u_{2|x_3=0} = 0 \quad \text{on } \Pi \mathcal{T}^\epsilon. \end{aligned} \tag{4.2}$$

Hence, the original 3d problem reduces to the study of two independent systems (with a Laplace and a Stokes equations), set in the 2d domain $\mathbb{T} \times (0,1)$. This change from a 3d to a 2d setting explains the change of scalings between Theorem 1 and Theorem 2.

To handle the Stokes equations (4.2), we proceed like in the previous section: in short, we adapt the homogenization techniques of [2, 3], dedicated to the Stokes flow across a periodic network of balls, set along an hypersurface. As mentioned before, the difference is the dimension of the domain. One must this time consider the 2d results of [3], about periodic network of disks along a line. For brevity, we do not give further details. We eventually obtain

the following limit system.

$$
\begin{aligned}
-\Delta_{2,3}\begin{pmatrix}\overline{u}_2\\ \overline{u}_3\end{pmatrix}+\nabla_{2,3}\overline{p}=\begin{pmatrix}f_2\\ f_3\end{pmatrix} \quad &\text{in } \mathbb{T}^1\times(0,1),\\
\nabla_{2,3}\cdot\begin{pmatrix}\overline{u}_2\\ \overline{u}_3\end{pmatrix}=0 \quad &\text{in } \mathbb{T}^1\times(0,1),\\
\overline{u}_{2,3}=0 \quad &\text{on } \mathbb{T}^1\times\{1\},\\
\overline{u}_3=0 \ &\text{on } \mathbb{T}^1\times\{0\},\\
\partial_3\overline{u}_2=\frac{2\pi}{C_0} \ &\text{on } \mathbb{T}^1\times\{0\}.
\end{aligned}
\tag{4.3}
$$

As regards the Laplace equation (4.1), the idea is exactly the same. Actually, the situation is even simpler, and has been analysed for a longer time. Namely, one may start from the work of Cioranescu and Murat [7], instead of [2, section 4]. Again, we leave the details to the reader. In our setting, the limit system is

$$
\begin{aligned}
-\Delta_{2,3}\bar{u}_1=f_1 \quad &\text{in } \mathbb{T}^1\times(0,1),\\
\bar{u}_1=0 \quad &\text{on } \mathbb{T}^1\times\{1\},\\
\partial_3\bar{u}_1=\frac{\pi}{C_0}\bar{u}_1 \ &\text{on } \mathbb{T}^1\times\{0\}.
\end{aligned}
\tag{4.4}
$$

We deduce from systems (4.4) and (4.3) that $\overline{u}=\overline{u}_{M_{riblets}}$, $M_{riblets}$ being given by (2.8). The sub-cases where $f=e_1$ or $f=e_2$ follow easily.

5 Numerical simulations

This section is devoted to simulations of system (2.1)-(2.2)-(2.3). For simplicity, we shall restrict to constant source term (average pressure gradient), say

$$f \ = \ 2e, \quad e\in \mathrm{span}(e_1,e_2).$$

The idea is to recover numerically the scalings for the slip length given in Theorems 1 and 2. However, to observe significant slip implies to consider very small scales: patches of size less than ϵ^2, in a grid of side ϵ. This forbids direct computations. To overcome this difficulty, we shall rely on a boundary layer approximation of the Stokes flow. Such approximation, often implicitly used in physics papers, has been fully justified in the context of wall laws: see [12, 8, 4] among many others.

The starting point is to write the exact solution u^ϵ as

$$u^\epsilon(x) \ = \ u^P(x) \ + \ \epsilon v^\epsilon(x/\epsilon)$$

where u^P is the reference Poiseuille flow, satisfying (2.1) with Dirichlet condition at both planes. Remind that

$$u^P(x) \ = \ -x_3(x_3-1)e.$$

Hence, $v^\epsilon = v^\epsilon(y)$ satisfies

$$\begin{aligned} -\Delta v + \nabla p = 0, \quad &\text{in } \mathbb{T}^2 \times (0,1), \\ \text{div } v = 0, \quad &\text{in } \mathbb{T}^2 \times (0,1), \\ v = 0, \quad &y_3 = \epsilon^{-1}, \\ v_3 = 0, \quad &y_3 = 0, \\ v_h = 0, \quad y \in \epsilon^{-1} T^\epsilon \times \{0\}, \quad &\partial_{y_3} v_h = -e, \quad y \in \epsilon^{-1}(T^\epsilon)^c \times \{0\} \end{aligned} \tag{5.1}$$

Note that no approximation has been made so far. It is then tempting to put the roof $y_3 = \epsilon^{-1}$ at infinity replacing $\mathbb{T}^2 \times (0, \epsilon^{-1})$ by $\mathbb{T}^2 \times \mathbb{R}_+$. However, it is well-known that the resulting problem is overdetermined. Namely, the boundary layer field $v^{\epsilon,bl}$ satisfying

$$\begin{aligned} -\Delta v + \nabla p = 0, \quad &\text{in } \mathbb{T}^2 \times \mathbb{R}_+, \\ \text{div } v = 0, \quad &\text{in } \mathbb{T}^2 \times \mathbb{R}_+, \\ v_3 = 0, \quad &y_3 = 0, \\ v_h = 0, \quad y \in \epsilon^{-1} T^\epsilon \times \{0\}, \quad &\partial_{y_3} v_h = -e, \quad y \in \epsilon^{-1}(T^\epsilon)^c \times \{0\} \end{aligned} \tag{5.2}$$

has constant horizontal average:

$$v_h^{\epsilon,\infty} := \int_{\mathbb{T}^2} v_h^{\epsilon,bl}(y) dy_1 dy_2$$

with respect to y_3. More precisely, it can be shown that

$$v^{\epsilon,bl} \to (v_h^{\epsilon,\infty}, 0)$$

exponentially fast as y_3 goes to infinity. Furthermore, by linearity of (5.2), one may denote $v_h^{\epsilon,\infty} = V^{\epsilon,\infty} e$ for a two by two matrix $V^{\epsilon,\infty}$. Then, one can show that $V^{\epsilon,\infty}$ is symmetric positive definite, with

$$V^{\epsilon,\infty} e \cdot e = \int_{\mathbb{T}^2 \times \mathbb{R}_+} |\nabla v^{\epsilon,bl}|^2.$$

Note that everything depends on ϵ, through the rescaled domain $\epsilon^{-1} T^\epsilon$ in (5.2).

To correct the "boundary layer constant" at infinity, one must add a macroscopic Couette flow. One ends up with

$$u^\epsilon \approx u^P(x) + \epsilon v^{\epsilon,bl}(x/\epsilon) - \epsilon x_3 (V^{\epsilon,\infty} e, 0)$$

Averaging in the small scale, we find

$$u^{\epsilon,h}|_{x_3=0} \approx \epsilon V^{\epsilon,\infty} e, \quad \partial_3 u^\epsilon|_{x_3=0} \approx \partial_3 u^P|_{x_3=0} \approx e.$$

We end up with the approximate boundary condition

$$u_h^\epsilon = \epsilon V^{\epsilon,\infty} \partial_3 u_h^\epsilon \quad \text{at } x_3 = 0. \tag{5.3}$$

On the basis of the previous reasoning, one can implement the following strategy for the numerical computation of the slip length:

- Compute numerically (say with $e = e_1$ and $e = e_2$) the solution of (5.2), in order to determine the matrix $V^{\epsilon,\infty}$.

- Check for the asymptotics of $\epsilon V^{\epsilon,\infty}$, for various shapes and sizes of the no-slip zone T^ϵ. This allows to make the comparison with theoretical results of Theorems 1 and 2. Indeed, sending ϵ to zero in (5.3) yields

$$\bar{u}_h \;=\; \lim_{\epsilon\to 0} (\epsilon V^{\epsilon,\infty})\, \partial_3 \bar{u}_h \quad \text{ at } \; x_3 = 0, \tag{5.4}$$

  so that the matrix M in the theorems satisfies $M^{-1} = \lim_{\epsilon\to 0} (\epsilon V^{\epsilon,\infty})$.

Numerical approximation of the matrix $V^{\epsilon,\infty}$. In the numerical simulations, we will solve the system (5.2) associated to different shapes of the no-slip zone T^ϵ: circular or rectangular patches, and riblets parallel or orthogonal to the flow. Let us first notice that for such configurations, the matrix $V^{\epsilon,\infty}$ is diagonal. Indeed, since the domain $\epsilon^{-1}T^\epsilon$ is symmetric with respect to the axis $\{y_2 = 1/2\}$, if we denote by v the solution to system (5.2) with $e = e_1$, then the vector field v^* defined by $v_i^*(y_1, y_2, y_3) = v_i(y_1, 1 - y_2, y_3)$, for $i = 1, 3$, and by $v_2^*(y_1, y_2, y_3) = -v_2(y_1, 1 - y_2, y_3)$, is also a solution. By uniqueness, we deduce that $v_2(y_1, 1 - y_2, y_3) = -v_2(y_1, y_2, y_3)$ for a.e. $(y_1, y_2, y_3) \in \mathbb{T}^2 \times \mathbb{R}_+$, which yields $V^{\epsilon,\infty} e_1 \cdot e_2 = 0$. By symmetry of $V^{\epsilon,\infty}$, we obtain also that $V^{\epsilon,\infty} e_2 \cdot e_1 = 0$

Consequently the boundary conditions satisfied by the horizontal components of the approximate solution to system (2.1)-(2.2)-(2.3) on $x_3 = 0$, simply writes:

$$u_i^\epsilon \;=\; \epsilon (V^{\epsilon,\infty} e_i \cdot e_i)\; \partial_3 u_i^\epsilon \quad \text{ at } \; x_3 = 0, \quad \text{for } i = 1, 2. \tag{5.5}$$

In the rest of this section, for $i = 1, 2$, the quantity $V^{\epsilon,\infty} e_i \cdot e_i$ will be refered to as the *average slip length* associated to our problem, in the direction e_i.

To compute an approximate value of the average slip length associated to system (5.2), we consider a truncated domain $\mathbb{T}^2 \times (0, H)$, for a given $H > 0$, and we introduce the solution w to the following problem:

$$\begin{aligned} -\Delta w + \nabla q &= 0, \quad \text{in } \; \mathbb{T}^2 \times (0, H), \\ \text{div } w &= 0, \quad \text{in } \; \mathbb{T}^2 \times (0, H), \\ \partial_{y_3} w - q\; e_3 &= 0, \quad y_3 = H, \\ w_3 &= 0, \quad y_3 = 0, \\ w_h = 0, \quad y \in \epsilon^{-1} T^\epsilon \times \{0\}, &\quad \partial_{y_3} w_h = -e, \quad y \in \epsilon^{-1} (T^\epsilon)^c \times \{0\} \end{aligned} \tag{5.6}$$

We solve problem (5.6) by a finite element method. We use P_2 elements for the velocity and P_1 elements for the pressure. The three-dimensional mesh of the fluid domain $\mathbb{T}^2 \times (0, H)$ is obtained by a constrained Delaunay tetrahedralization. The incompressibility condition is treated by a Lagrange multiplier (see [10], [11]).

Given two approximate solutions w_{app}^1, w_{app}^2 of system (5.6), associated respectively to $e = e_1$ and $e = e_2$, we define the numerical approximation $V_{app}^{\epsilon,\infty}$ of the matrix $V^{\epsilon,\infty}$, by the following formula:

$$V_{app}^{\epsilon,\infty} e_i \cdot e_j := \int_{\mathbb{T}^2} w_{app}^i(y_1, y_2, H) \cdot e_j \; dy_1 dy_2, \quad \text{for } i, j = 1, 2.$$

By analogy with formula (5.5), for $i = 1, 2$, the *approximate average slip length* in direction e_i is then defined by $V_{app}^{\epsilon,\infty} e_i \cdot e_i$.

Finally, we introduce the *solid fraction* ϕ_s^ϵ, which is defined by the relative area of the no-slip zone T^ϵ in the elementary square of size ϵ (or equivalently, by the area of the rescaled no-slip domain $\epsilon^{-1}T^\epsilon$). Using definitions (2.4)-(2.5), ϕ_s^ϵ is given by the following expressions:

- in the case of patches, $\phi_s^\epsilon = \left(\frac{a_\epsilon}{\epsilon}\right)^2 |T|$, where $|T|$ stands for the area of the domain T;
- in the case of riblets, $\phi_s^\epsilon = \frac{a_\epsilon}{\epsilon}|I|$, where $|I|$ stands for the length of the interval I.

Notice that system (5.2) is completely determined by ϕ_s^ϵ and by the domain T (in the case of patches) or the union of intervals I (in the case of riblets).

Computation of the average slip length, in the case of patches. In the case of patches, we have plotted $V_{app}^{\epsilon,\infty} e_1 \cdot e_1$ against $1/\sqrt{\phi_s^\epsilon}$, considering circular and squared patches (see Figure 4). We observe that the dependency is affine, and a linear regression gives the relation $V_{app}^{\epsilon,\infty} e_1 \cdot e_1 \approx \alpha/\sqrt{\phi_s^\epsilon} + \beta$, with $\alpha = 0.322$, $\beta = -0.429$ in the case of the disk, and $\alpha = 0.311$, $\beta = -0.422$ in the case of the square. Note that these coefficients are very close to the ones obtained by Ybert *et al.* [17]. Consequently, since $\lim_{\epsilon\to 0} \phi_s^\epsilon = 0$,

$$V_{app}^{\epsilon,\infty} e_1 \cdot e_1 \sim \frac{\alpha}{\sqrt{\phi_s^\epsilon}} \quad \text{as } \epsilon \to 0. \tag{5.7}$$

To compare this numerical result with the theoretical result given by Theorem 1, let us consider the critical case $a_\epsilon/\epsilon^2 \to C_0 > 0$. In that case, there exists a two by two matrix M_0, depending on the pattern T, such that $\lim_{\epsilon\to 0} \epsilon V^{\epsilon,\infty} = \frac{1}{C_0} M_0^{-1}$. For circular or squared patterns centered in the unit square, as observed above, the matrices $V^{\epsilon,\infty}$, and consequently the matrix M_0, are diagonal. Moreover, since these patterns are invariant by a rotation of angle $\pi/2$, one can easily see that the corresponding matrix $V^{\epsilon,\infty}$ satisfies $V^{\epsilon,\infty} e_1 \cdot e_1 = V^{\epsilon,\infty} e_2 \cdot e_2$. Consequently, there exists $\lambda_0 > 0$ such that $M_0 = \begin{pmatrix} \lambda_0 & 0 \\ 0 & \lambda_0 \end{pmatrix}$, and the following relation holds:

$$\lim_{\epsilon\to 0} \epsilon V^{\epsilon,\infty} e_1 \cdot e_1 = \frac{1}{C_0\, \lambda_0}.$$

Besides, using the definition of ϕ_s^ϵ in the case of patches, the asymptotic relation (5.7) yields

$$\lim_{\epsilon\to 0} \epsilon V_{app}^{\epsilon,\infty} e_1 \cdot e_1 = \frac{\alpha}{C_0\sqrt{|T|}}.$$

Thus, the numerical value of the slip length $\alpha/(C_0\sqrt{|T|})$, that can be deduced from the asymptotic behavior (5.7) in the critical case, is consistent with Theorem 1. The coefficient of the matrix M_0 can be approximated by $\lambda_0 \approx \sqrt{|T|}/\alpha$.

We notice that the results concerning the sub-critical and super-critical cases can also be retrieved, at least formally, from relation (5.7). Indeed, since $\epsilon/\sqrt{\phi_s^\epsilon} = \epsilon^2/(a_\epsilon\sqrt{|T|})$, we obtain in the sub-critical case: $\lim_{\epsilon\to 0} \epsilon V_{app}^{\epsilon,\infty} e_1 \cdot e_1 = +\infty$, which corresponds formally to an infinite slip length in the e_1 direction, that is, a perfect slip condition. In the same manner, in the super-critical case, we obtain $\lim_{\epsilon\to 0} \epsilon V_{app}^{\epsilon,\infty} e_1 \cdot e_1 = 0$, which corresponds to adherence in the e_1 direction.

Computation of the average slip length, in the case of riblets. In that case, exact computations are available in the literature, that give the average slip lengths in the e_1 and e_2 direction as a function of the solid fraction ϕ_s^ϵ (see for instance [14]):

$$V^{\epsilon,\infty}e_1 \cdot e_1 = -\ln\left[\cos\left(\frac{\pi}{2}(1-\phi_s^\epsilon)\right)\right]/\pi, \quad V^{\epsilon,\infty}e_2 \cdot e_2 = -\ln\left[\cos\left(\frac{\pi}{2}(1-\phi_s^\epsilon)\right)\right]/(2\pi). \quad (5.8)$$

We have plotted in Figure 5 the computed value of the average slip lengths $V_{app}^{\epsilon,\infty}e_1 \cdot e_1$ and $V_{app}^{\epsilon,\infty}e_2 \cdot e_2$, against ϕ_s^ϵ, as well as the exact values defined by formulas (5.8). We observe that the numerical values are close to the expected ones.

Once again, formulas (5.8) and the numerical behavior of the average slip length shown in Figure 5, are consistent with the theoretical results of Theorem 2. Indeed, in the critical case $\lim_{\epsilon\to 0} -\epsilon\ln(a_\epsilon) = C_0 > 0$, using the expression $\phi_s^\epsilon = (a_\epsilon|I|)/\epsilon$, one obtains by a straightforward computation that $\epsilon\ln\left[\cos\left(\frac{\pi}{2}(1-\phi_s^\epsilon)\right)\right] \to -C_0$ as $\epsilon \to$. Consequently, the slip length in the directions e_1 and e_2 are respectively given by

$$\lim_{\epsilon\to 0}\epsilon V^{\epsilon,\infty}e_1 \cdot e_1 = \frac{C_0}{\pi}, \quad \lim_{\epsilon\to 0}\epsilon V^{\epsilon,\infty}e_2 \cdot e_2 = \frac{C_0}{2\pi}.$$

Influence of the shape of the no-slip area: comparative results. In order to provide a comparison between the efficiency of patches and riblets in terms of slip length, we consider the slip length in the direction of the constant pressure gradient $f = 2e_i$, with $i = 1$ or $i = 2$. For circular or squared patterns, the average slip length is given by $V^{\epsilon,\infty}e_1 \cdot e_1$. In the case of riblets, we consider two configurations of physical interest:

- riblets parallel to the flow: $f = 2e_1$, the average slip length is defined by $V^{\epsilon,\infty}e_1 \cdot e_1$;
- riblets orthogonal to the flow: $f = 2e_2$, the average slip length is $V^{\epsilon,\infty}e_2 \cdot e_2$.

The results are plotted in Figure 6. As stated in Remark 3, page 5, these numerical results confirm that the riblets parallel to the flow are not necessarily optimal. Indeed, if the solid fraction ϕ_s^ϵ is small enough, say $\phi_s^\epsilon < 0.1$, the circular or squared patches produce a superior slip length.

To estimate the influence of the shape of the pattern on the slip length, we have considered families of rectangles of fixed area ϕ_s^ϵ, that are centered in the unit square. For $\phi_s^\epsilon = 0.01, 0.04, 0.09$ we have computed the average slip length $V_{app}^{\epsilon,\infty}e_1 \cdot e_1$, in the direction e_1, associated to each of these rectangular patterns. The results are plotted in figure 7, against the dimension L of each rectangular pattern, in the e_1 direction. For each solid fraction ϕ_s^ϵ, the extremal values associated to $L = \phi_s^\epsilon$ and $L = 1$, correspond respectively to a riblet orthogonal to the flow, and parallel to the flow.

We notice that, for each family of rectangular patterns of fixed area, the riblet orthogonal to the flow provides always the smallest average slip length. As already mentionned, the riblet parallel to the flow is not optimal, especially for small values of the solid fraction $\phi_s^\epsilon = 0.01$, $\phi_s^\epsilon = 0.04$. In that cases, the curves present a unique maximum, and the associated optimal size L of the rectangle is slightly superior to the size $\sqrt{\phi_s^\epsilon}$ of the square of same area. For these values of the solid fraction, the optimal rectangular pattern will present a certain anisotropy in the direction of the flow.

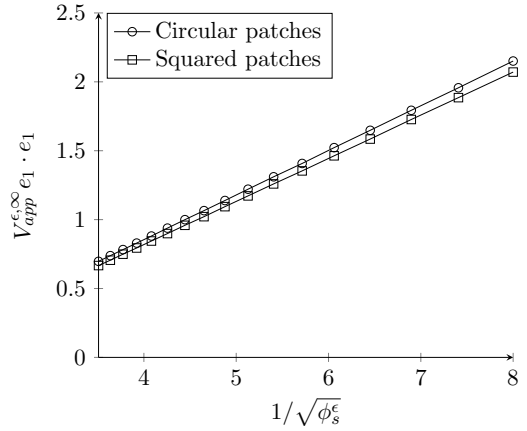

Figure 4: Numerical value of the average slip length $V_{app}^{\epsilon,\infty} e_1 \cdot e_1$ plotted against $1/\sqrt{\phi_s^\epsilon}$, for circular patches and squared patches.

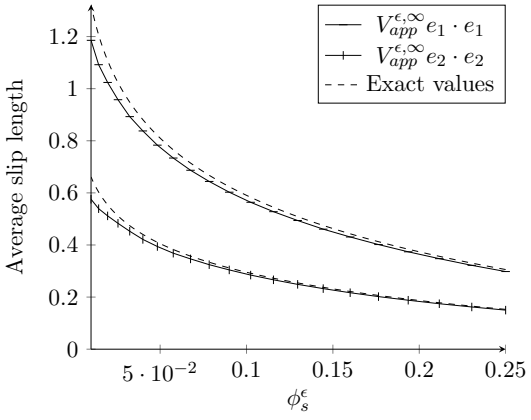

Figure 5: Numerical values of the average slip lengths $V_{app}^{\epsilon,\infty} e_1 \cdot e_1$ and $V_{app}^{\epsilon,\infty} e_2 \cdot e_2$, plotted against ϕ_s^ϵ, in the case of riblets. The dashed lines represent the exact value of the average slip lengths, defined by formulas (5.8).

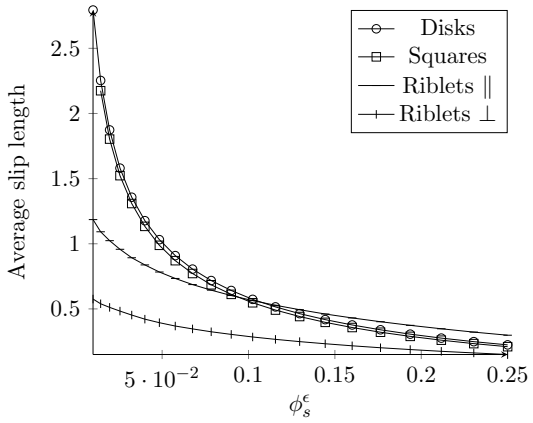

Figure 6: Average slip length in the direction of the flow, in the case of circular patches, squared patches and riblets parallel and orthogonal to the flow.

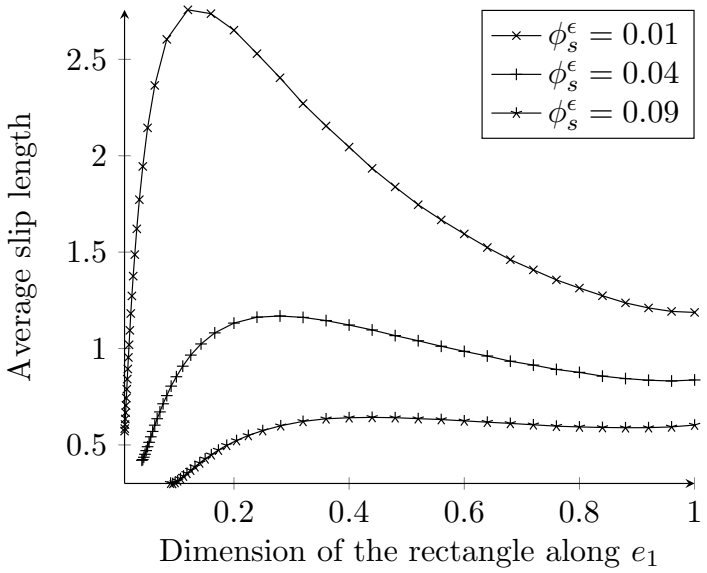

Figure 7: Numerical values of the average slip length $V_{app}^{\epsilon,\infty} e_1 \cdot e_1$, produced by rectangular patterns of given area $\phi_s^\epsilon \in \{0.01, 0.04, 0.09\}$, and plotted against the dimension L of the rectangle in the e_1 direction. The extremal value $L = \phi_s^\epsilon$ (resp. $L = 1$) corresponds to the riblet orthogonal to the flow (resp. parallel to the flow).

Appendix: proof of inequality (3.2)

To obtain inequality (3.2), it is enough to prove that for every $k \in [|0, \epsilon^{-1}|]^2$,

$$\int_{S_k^\epsilon \times \{0\}} |u^\epsilon|^2 \;\leq\; \eta(\epsilon) \int_{B_k^{\epsilon,+}} |\nabla u^\epsilon|^2 \qquad \forall 0 < \epsilon < \epsilon_0. \tag{5.9}$$

A summation over $k \in [|0, \epsilon^{-1}|]^2$ then leads to inequality (3.2).

Let $k \in [|0, \epsilon^{-1}|]^2$. By rescaling the trace inequality in the half cube $[0,1]^2 \times [0, \frac{1}{2}]$, we obtain the existence of a constant $C > 0$ such that

$$\int_{S_k^\epsilon \times \{0\}} |u^\epsilon|^2 \leq C \left(\epsilon \int_{P_k^{\epsilon,+}} |\nabla u^\epsilon|^2 + \frac{1}{\epsilon} \int_{P_k^{\epsilon,+}} |u^\epsilon|^2 \right). \tag{5.10}$$

To estimate the L^2 norm of u^ϵ by the L^2 norm of its gradient, we adapt [3, Lemma 3.4.1] to our bidimensional framework. We denote by B_k^ϵ the ball circumscribing the cube P_k^ϵ. Of course, the upper half-cube $P_k^{\epsilon,+}$ is contained in the upper half-ball $B_k^{\epsilon,+}$. Moreover, since the model no-slip zone T contains a disk of radius α centered at the origin, each elementary no-slip pattern $\epsilon k + T^\epsilon$ contains a disk of radius $a_\epsilon \alpha$, centered in the square S_k^ϵ. Let $\tilde{B}_k^\epsilon$ be the ball of same center and radius, and $\tilde{B}_k^{\epsilon,+}$ be the corresponding half ball. With this notation, we can write

$$\int_{P_k^{\epsilon,+}} |u^\epsilon|^2 \leq \int_{B_k^{\epsilon,+} \setminus \tilde{B}_k^{\epsilon,+}} |u^\epsilon|^2 + \int_{\tilde{B}_k^{\epsilon,+}} |u^\epsilon|^2.$$

To estimate the contribution of the exterior part $B_k^{\epsilon,+} \setminus \tilde{B}_k^{\epsilon,+}$, we use spherical coordinates (ρ, ϕ, θ) centered at point $\epsilon k + (\frac{\epsilon}{2}, \frac{\epsilon}{2}, 0)$. The radius of B_k^ϵ being equal to $\frac{\epsilon\sqrt{3}}{2}$, integrating along rays, we get for every r', r such that $0 < r' < a_\epsilon \alpha < r < \frac{\epsilon\sqrt{3}}{2}$,

$$u^\epsilon(r, \phi, \theta) = u^\epsilon(r', \phi, \theta) + \int_{r'}^{r} \partial_\rho u^\epsilon(\rho, \phi, \theta) \mathrm{d}\rho,$$

which yields

$$|u^\epsilon(r, \phi, \theta)|^2 \leq 2|u^\epsilon(r', \phi, \theta)|^2 + 2 \left(\int_{r'}^{r} \partial_\rho u^\epsilon(\rho, \phi, \theta) \mathrm{d}\rho \right)^2.$$

Multiplying last inequality by $r^2 (r')^2 \sin\theta$ and integrating on $r' \in (0, a_\epsilon \alpha)$, $r \in (a_\epsilon \alpha, \frac{\epsilon\sqrt{3}}{2})$, $\phi \in (0, 2\pi)$, $\theta \in (0, \pi/2)$, we obtain the inequality

$$I^\epsilon \leq 2J^\epsilon + 2K^\epsilon \tag{5.11}$$

where the integrals I^ϵ, J^ϵ, K^ϵ are respectively defined by

$$I^\epsilon = \int_{r'=0}^{a_\epsilon \alpha} \int_{r=a_\epsilon \alpha}^{\frac{\epsilon\sqrt{3}}{2}} \int_\theta \int_\phi |u(r, \phi, \theta)|^2 r^2 (r')^2 \sin\theta \; \mathrm{d}\theta \; \mathrm{d}\phi \; \mathrm{d}r \; \mathrm{d}r',$$

$$J^\epsilon = \int_{r'=0}^{a_\epsilon \alpha} \int_{r=a_\epsilon \alpha}^{\frac{\epsilon\sqrt{3}}{2}} \int_\theta \int_\phi |u(r', \phi, \theta)|^2 r^2 (r')^2 \sin\theta \; \mathrm{d}\theta \; \mathrm{d}\phi \; \mathrm{d}r \; \mathrm{d}r',$$

$$K^\epsilon = \int_{r'=0}^{a_\epsilon \alpha} \int_{r=a_\epsilon \alpha}^{\frac{\epsilon\sqrt{3}}{2}} \int_\theta \int_\phi \left(\int_{r'}^{r} \partial_\rho u^\epsilon(\rho, \phi, \theta) \mathrm{d}\rho \right)^2 r^2 (r')^2 \sin\theta \; \mathrm{d}\theta \; \mathrm{d}\phi \; \mathrm{d}r \; \mathrm{d}r'.$$

By Fubini theorem,

$$I^\epsilon = \left(\int_0^{a_\epsilon\alpha} (r')^2 \mathrm{d}r'\right)\left(\int_{r=a_\epsilon\alpha}^{\frac{\epsilon\sqrt{3}}{2}} \int_\theta \int_\phi |u(r,\phi,\theta)|^2 r^2 \sin\theta \ \mathrm{d}\theta \ \mathrm{d}\phi \ \mathrm{d}r\right) = \frac{a_\epsilon^3\alpha^3}{3} \int_{B_k^{\epsilon,+}\setminus\tilde{B}_k^{\epsilon,+}} |u^\epsilon|^2,$$

and by an analogous computation,

$$J^\epsilon = \left(\epsilon^3 \frac{3\sqrt{3}}{8} - \frac{a_\epsilon^3\alpha^3}{3}\right) \int_{\tilde{B}_k^{\epsilon,+}} |u^\epsilon|^2.$$

By Schwarz inequality,

$$\left(\int_{r'}^r \partial_\rho u^\epsilon \mathrm{d}\rho\right)^2 \leq \left(\int_{r'}^r \frac{1}{\rho^2}\mathrm{d}\rho\right)\left(\int_{r'}^r \rho^2 |\partial_\rho u^\epsilon|^2 \mathrm{d}\rho\right) \leq \frac{1}{r'}\int_{r'}^r \rho^2 |\partial_\rho u^\epsilon|^2 \mathrm{d}\rho,$$

which yields

$$K^\epsilon \leq \left(\int_{a_\epsilon\alpha}^{\frac{\epsilon\sqrt{3}}{2}} r^2 \ \mathrm{d}r\right)\left(\int_0^{a_\epsilon\alpha} r' \ \mathrm{d}r'\right)\left(\int_{B_k^{\epsilon,+}} |\nabla u^\epsilon|^2\right) \leq \frac{3\sqrt{3}}{16} a_\epsilon^2\alpha^2\epsilon^3 \int_{B_k^{\epsilon,+}} |\nabla u^\epsilon|^2.$$

Consequently, inequality (5.11) leads to

$$\int_{B_k^{\epsilon,+}\setminus\tilde{B}_k^{\epsilon,+}} |u^\epsilon|^2 \leq \frac{9\sqrt{3}}{8}\frac{\epsilon^3}{a_\epsilon\alpha}\left(\frac{2}{a_\epsilon^2\alpha^2}\int_{\tilde{B}_k^{\epsilon,+}} |u^\epsilon|^2 + \int_{B_k^{\epsilon,+}} |\nabla u^\epsilon|^2\right). \tag{5.12}$$

Since u^ϵ vanishes on $\tilde{B}_k^{\epsilon,+} \cap (\mathbb{R}^2 \times \{0\})$, using Poincaré inequality in a cylinder of height $a_\epsilon\alpha$, we obtain the following estimate:

$$\int_{\tilde{B}_k^{\epsilon,+}} |u^\epsilon|^2 \leq a_\epsilon^2\alpha^2 \int_{B_k^{\epsilon,+}} |\nabla u^\epsilon|^2.$$

Injecting this inequality into estimate (5.12), we obtain:

$$\int_{B_k^{\epsilon,+}\setminus\tilde{B}_k^{\epsilon,+}} |u^\epsilon|^2 \leq \frac{27\sqrt{3}\epsilon^3}{a_\epsilon\alpha} \int_{B_k^{\epsilon,+}} |\nabla u^\epsilon|^2,$$

and summing these two inequalities, we get

$$\int_{B_k^{\epsilon,+}} |u^\epsilon|^2 \leq \left(a_\epsilon^2\alpha^2 + \frac{27\sqrt{3}\epsilon^3}{a_\epsilon\alpha}\right) \int_{B_k^{\epsilon,+}} |\nabla u^\epsilon|^2.$$

Finally, using inequality (5.10), we obtain estimate (5.9), where $\eta(\epsilon)$ is defined by

$$\eta(\epsilon) = C\left(\epsilon + \frac{a_\epsilon^2\alpha^2}{\epsilon} + \frac{27\sqrt{3}\epsilon^2}{a_\epsilon\alpha}\right),$$

and converges to 0 as $\epsilon \to 0$, since $a_\epsilon < \epsilon$ and $a_\epsilon \gg \epsilon^2$. □

References

[1] Yves Achdou, O. Pironneau, and F. Valentin, *Effective boundary conditions for laminar flows over periodic rough boundaries*, J. Comput. Phys. **147** (1998), no. 1, 187–218. MR 1657773 (99j:76086)

[2] Grégoire Allaire, *Homogenization of the Navier-Stokes equations in open sets perforated with tiny holes. I. Abstract framework, a volume distribution of holes*, Arch. Rational Mech. Anal. **113** (1990), no. 3, 209–259.

[3] ———, *Homogenization of the Navier-Stokes equations in open sets perforated with tiny holes. II. Noncritical sizes of the holes for a volume distribution and a surface distribution of holes*, Arch. Rational Mech. Anal. **113** (1990), no. 3, 261–298.

[4] Youcef Amirat, Didier Bresch, Jérôme Lemoine, and Jacques Simon, *Effect of rugosity on a flow governed by stationary Navier-Stokes equations*, Quart. Appl. Math. **59** (2001), no. 4, 769–785. MR 1866556 (2002g:76036)

[5] Arnaud Basson and David Gérard-Varet, *Wall laws for fluid flows at a boundary with random roughness*, Comm. Pure Appl. Math. **61** (2008), no. 7, 941–987. MR 2410410 (2009h:76055)

[6] D. Bucur, A.-L. Dalibard, and D. Gerard-Varet, *Wall laws for viscous fluids near rough surfaces*, ESAIM Proc **37** (2012), 117–135.

[7] D. Cioranescu and F. Murat, *Un terme étrange venu d'ailleurs*, Nonlinear partial differential equations and their applications. Collège de France Seminar, Vol. II (Paris, 1979/1980), Res. Notes in Math., vol. 60, Pitman, Boston, Mass., 1982, pp. 98–138, 389–390. MR 652509 (84e:35039a)

[8] Anne-Laure Dalibard and David Gérard-Varet, *Effective boundary condition at a rough surface starting from a slip condition*, J. Differential Equations **251** (2011), no. 12, 3450–3487. MR 2837691 (2012k:35031)

[9] G. P. Galdi, *An introduction to the mathematical theory of the Navier-Stokes equations*, second ed., Springer Monographs in Mathematics, Springer, New York, 2011, Steady-state problems. MR 2808162 (2012g:35233)

[10] Vivette Girault and Pierre-Arnaud Raviart, *Finite element methods for Navier-Stokes equations*, Springer Series in Computational Mathematics, vol. 5, Springer-Verlag, Berlin, 1986, Theory and algorithms. MR 851383 (88b:65129)

[11] Kazufumi Ito and Karl Kunisch, *Lagrange multiplier approach to variational problems and applications*, Advances in Design and Control, vol. 15, Society for Industrial and Applied Mathematics (SIAM), Philadelphia, PA, 2008. MR 2441683 (2009g:49001)

[12] Willi Jäger and Andro Mikelić, *On the roughness-induced effective boundary conditions for an incompressible viscous flow*, J. Differential Equations **170** (2001), no. 1, 96–122. MR 1813101 (2002b:76049)

[13] E. Lauga, M.P. Brenner, and H.A. Stone, *Microfluidics: The no-slip boundary condition*, Handbook of Experimental Fluid Dynamics,C. Tropea, A. Yarin, J. F. Foss (Eds.), Springer, 2007, p. 123601.

[14] John R. Philip, *Flows satisfying mixed no-slip and no-shear conditions*, Z. Angew Math. Phys. **23** (1972), 353–372. MR 0321415 (47 #9948)

[15] V. A. Solonnikov and V. E. Ščadilov, *On a boundary value problem for a stationary system of Navier-Stokes equations*, Proc. Steklov Inst. Math. **125** (1973), 186–199.

[16] O. Vinogradova and G. Yakubov, *Surface roughness and hydrodynamic boundary conditions*, Phys. Rev. E (2006), 479–487.

[17] C. Ybert, C. Barentin, C. Cottin-Bizonne, P. Joseph, and Bocquet L., *Achieving large slip with superhydrophobic surfaces: Scaling laws for generic geometries*, Physics of fluids **19** (2007), 123601.